International Journal of Research & Social Sciences

Volume: 06 Issue: 02 (2026)
www.ijrss.com

Influence of Sand-Layer Interfaces on the Penetration Energy of Composite Offshore Bucket Foundations

Haruka Morita

Department of Mechanical Engineering, Faculty of Science and Technology, Keio University, Tokyo, Japan

Abstract:
The rapid expansion of offshore wind energy into deeper waters and more complex geological environments has necessitated the development of advanced foundation concepts, such as composite offshore bucket foundations. The installation of these structures often encounters highly stratified soil profiles, where the presence of distinct sand-layer interfaces significantly alters penetration resistance and the total energy required for successful installation. This paper investigates the influence of varying sand-layer interfaces on the penetration energy of composite offshore bucket foundations through a comprehensive synthesis of theoretical formulations, scaled physical modeling, and advanced numerical simulations. By isolating the interface effects between loose and dense sand layers, the study systematically evaluates the evolution of penetration resistance, the formation of soil plugs, and the localized stress distribution mechanisms at the interface transition zone. The findings indicate that penetration energy does not increase linearly across interfaces but exhibits a pronounced gradient highly dependent on the relative density contrast and the depth of the interface. This non-linear energy accumulation poses substantial risks for premature refusal during installation. A predictive framework incorporating these interface effects is proposed, offering a refined calculation method for penetration energy in heterogeneous marine soils. The results provide critical insights for optimizing the structural design and installation protocols of offshore bucket foundations in complex geotechnical environments.

Keywords: *Composite Bucket Foundation, Sand-Layer Interface, Penetration Energy, Offshore Wind Turbine*

INTRODUCTION

1.1 Background on Offshore Renewable Energy and Foundation Systems

The global transition toward sustainable and renewable energy sources has dramatically accelerated the development and deployment of offshore wind farms. As onshore wind locations reach saturation and nearshore shallow-water sites become fully utilized, the offshore wind industry is inexorably moving toward deeper waters. These deeper marine environments offer the advantage of higher, more consistent wind speeds, which translate into significantly greater energy yields. However, the migration into deeper waters introduces profound engineering challenges, primarily related to the design, transportation, and installation of the foundational structures that must securely anchor the massive offshore wind turbines to the seabed. Traditional foundation systems, such as monopiles and jacket structures, have been deployed extensively in shallow to

transitional waters [1]. While effective, the installation of monopiles requires heavy hydraulic hammering, which generates substantial underwater noise pollution that is detrimental to marine life and demands highly specialized, expensive heavy-lift vessels. Furthermore, as water depth increases, the required diameter and length of monopiles increase exponentially, pushing the boundaries of current manufacturing and transportation capabilities. In response to these significant technical and economic limitations, the offshore geotechnical engineering community has developed alternative foundation concepts, among which the composite offshore bucket foundation has emerged as a highly promising solution. The composite offshore bucket foundation combines the principles of traditional suction caissons with enhanced structural rigidity and load-bearing geometries, allowing it to support larger turbines in more challenging environments while mitigating the environmental and economic drawbacks of driven piles [2].

1.2 The Mechanism and Challenges of Bucket Foundation Installation

The fundamental appeal of the composite offshore bucket foundation lies in its innovative installation process. Unlike driven piles, the bucket foundation is initially lowered to the seabed where it penetrates the surficial soil layers under its own massive self-weight [3]. Once the foundation reaches a state of equilibrium where the bearing capacity of the soil equals the buoyant weight of the structure, active installation commences. This active phase involves pumping water out of the sealed interior cavity of the bucket, thereby creating a differential pressure—or suction—between the hydrostatic pressure of the surrounding seawater and the reduced pressure inside the bucket. This pressure differential acts as a massive downward driving force, simultaneously inducing a downward flow of water through the soil plug within the bucket. In permeable soils such as sand, this downward seepage flow significantly reduces the effective stress of the soil plug at the tip of the bucket skirt, effectively degrading the penetration resistance and allowing the foundation to advance smoothly into the seabed. However, this elegantly simple mechanism becomes highly complex in highly stratified marine soils, which are the norm rather than the exception in many offshore environments. Marine deposits are frequently characterized by alternating layers of varying grain size, mineralogy, and relative density, formed over millennia by fluctuating sea levels, glacial activities, and shifting ocean currents. When a composite bucket foundation penetrates through a homogeneous soil layer, the penetration resistance and the corresponding energy required for installation increase at a relatively predictable rate. However, when the foundation skirt encounters an interface between two distinct soil layers—particularly interfaces between different strata of sand with varying relative densities—the installation dynamics are subjected to sudden and severe disruptions [4].

1.3 The Significance of Penetration Energy and Interface Effects

The concept of penetration energy is central to evaluating the feasibility and safety of offshore bucket foundation installation. Penetration energy represents the cumulative mechanical work required to advance the foundation from the seabed surface to its final design depth. It is calculated by integrating the penetration resistance over the total installation depth. Accurate estimation of this energy is absolutely critical; if the available driving energy (derived from self-weight and maximum allowable suction pressure) is insufficient to overcome the required penetration energy, the foundation will experience premature refusal, leaving it partially installed and structurally compromised. The presence of a sand-layer interface, such as a transition from a loose, highly permeable superficial sand deposit to an underlying dense, less permeable sand layer, dramatically alters the accumulation of penetration energy [5]. At such interfaces, the simplified assumptions of soil mechanics utilized for homogeneous deposits break down. The transition zone induces complex stress redistribution, localized variations in the seepage field, and alterations in the friction mobilization along the bucket skirt. Consequently, the penetration energy often exhibits a highly non-linear spike as the foundation crosses the interface, an anomaly that traditional

predictive models frequently fail to capture. Understanding the influence of these sand-layer interfaces on the penetration energy is therefore not merely a theoretical curiosity, but a critical imperative for the safe, predictable, and economical installation of composite offshore bucket foundations. This paper aims to meticulously dissect these interface effects through a combined approach of theoretical analysis, scaled physical experimentation, and rigorous computational modeling, thereby providing a comprehensive understanding of energy accumulation mechanisms during complex soil penetration [6].

2. Literature Review and Background

2.1 Evolution of Suction Foundation Geotechnics

The fundamental principles of suction-assisted penetration have been investigated extensively over the past few decades, initially driven by the offshore oil and gas industry for mooring floating platforms. Early foundational studies focused primarily on homogeneous clay deposits, where installation is governed entirely by undrained shear strength and where the application of suction does not significantly alter the effective stress state of the soil ahead of the foundation tip [7]. In these fine-grained environments, penetration resistance is largely a function of soil remolding and adhesion along the foundation walls. As the application of bucket foundations expanded into sandy marine environments for wind energy, researchers began to explore the profound effects of seepage-induced effective stress reduction. Studies demonstrated that the application of internal underpressure generates an upward hydraulic gradient within the soil plug inside the foundation. This gradient reduces the effective vertical stress, loosening the sand and drastically reducing the tip resistance [8]. However, this seepage mechanism introduces its own set of risks, most notably the potential for piping or boiling if the critical hydraulic gradient is exceeded, which can lead to the formation of channels, loss of bearing capacity, and excessive settlement [9]. Extensive laboratory testing and field trials established operational boundaries for suction pressures in homogeneous sands, ensuring that maximum penetration could be achieved without inducing catastrophic soil failure. These foundational studies provided the basis for the classical calculation methods of penetration resistance, which sum the internal and external skin friction with the tip resistance, appropriately modified by the seepage effects [10].

2.2 Behavior of Foundations in Layered Marine Soils

While the mechanics of bucket installation in homogeneous soils are reasonably well understood, the transition to layered soil profiles introduced a high degree of complexity that remains an active area of research. Offshore site investigations consistently reveal stratified profiles comprising alternating layers of clay, silt, and sand. Initial research into layered soils primarily addressed clay-over-sand or sand-over-clay profiles. In clay-over-sand conditions, the primary challenge is achieving sufficient penetration into the underlying sand to ensure stability, given that the suction applied in the upper clay layer cannot generate the necessary seepage flow to soften the underlying sand. Conversely, in sand-over-clay profiles, there is a risk that the highly permeable sand allows rapid dissipation of underpressure, making it difficult to generate enough suction to penetrate the underlying stiffer clay [11]. Recent attention has shifted toward the even more complex scenario of sand-over-sand interfaces, where varying relative densities, particle size distributions, and mineralogies create subtle yet impactful variations in geotechnical behavior. Research has indicated that when a foundation approaches an interface between a loose overlying sand and a dense underlying sand, the penetration resistance begins to increase well before the physical boundary is reached. This phenomenon is attributed to the formation of a stress bulb ahead of the penetrating tip, which interacts with the stiffer underlying layer and forces premature mobilization of strength [12]. The extent of this influence zone and its corresponding impact on penetration energy remains a subject of considerable debate and investigation [13].

2.3 Penetration Energy and Current Knowledge Gaps

The specific metric of penetration energy has historically been overshadowed by the focus on peak penetration resistance. However, from an installation mechanics perspective, energy is often the more critical parameter. The energy required reflects not only the peak resistance encountered but the sustained effort needed to drive the foundation through challenging zones, dictating the required capacity of the suction pump systems and the structural fatigue imposed on the foundation itself [14]. Current predictive models often calculate total energy by simply integrating resistance curves derived from homogeneous layer assumptions, effectively treating interfaces as abrupt, instantaneous changes in material properties. This simplified approach completely ignores the transitional mechanics, the development of the stress bulb, and the alteration of seepage patterns at the interface, leading to significant discrepancies between predicted and actual installation energies. Furthermore, the introduction of the composite offshore bucket foundation, which features internal bulkheads, varying skirt thicknesses, and complex transition geometries between the bucket and the superstructure, exacerbates these interface effects. The interaction between these structural complexities and the sand-layer interface creates highly localized zones of energy dissipation that are not captured by simplified analytical models [15]. Therefore, a critical knowledge gap exists regarding the precise formulation of penetration energy for composite foundations in highly stratified sand profiles. Addressing this gap requires a multifaceted approach that captures both the macroscopic energy accumulation and the microscopic soil-structure interaction mechanisms occurring at the interface transition zone.

3. Theoretical Framework and Penetration Mechanisms

3.1 Kinematics of Penetration in Granular Media

The theoretical conceptualization of a composite offshore bucket foundation penetrating through a granular medium is fundamentally a problem of large-deformation, large-strain soil-structure interaction. As the leading edge of the bucket skirt is forced into the seabed, it displaces a volume of sand equal to its own volume, inducing a complex field of radial and vertical displacements. In an ideal, homogeneous state, this displacement induces a stress field that can be analyzed using cavity expansion theory or classical bearing capacity formulations. The total resistance to penetration at any given depth is the summation of three distinct components: the frictional resistance along the external surface of the skirt, the frictional resistance along the internal surface of the skirt, and the end-bearing resistance at the annular tip of the skirt [16]. In fully drained conditions without the application of suction, the effective stresses governing both friction and end-bearing increase linearly with depth. However, during active suction installation, the applied underpressure alters the pore water pressure regime. The downward flow of water outside the bucket increases the effective stress and, consequently, the external friction. Conversely, the upward flow inside the bucket decreases the effective stress, dramatically reducing internal friction and tip resistance. The total penetration resistance force can be expressed as a depth-dependent function.

$$F_p = \sum_{i=1}^{n} (\tau_{ext,i} A_{ext,i} + \tau_{int,i} A_{int,i}) + q_{tip} A_{tip}$$

Where the internal and external shear stresses and the tip resistance are intricately linked to the dynamic effective stress state modified by the seepage velocity field.

3.2 Mechanics of the Sand-Layer Interface Transition

The fundamental assumptions governing the aforementioned mechanisms are severely challenged when the penetrating structure approaches a geological interface. Consider a scenario where a composite bucket foundation is penetrating a loose sand layer and approaching an interface with a significantly denser sand layer. As the skirt tip progresses downward, it carries with it a localized zone of compacted soil, often referred to as a "false tip" or stress bulb. The dimensions and intensity of this stress bulb depend on the geometry of the skirt tip and the friction angle of the

soil. As the stress bulb impinges upon the dense sand layer below, the boundary conditions of the penetrating zone change from a semi-infinite uniform half-space to a constrained layered system. The stiffer underlying material restricts the downward and radial displacement of the soil particles within the stress bulb, forcing the failure surfaces to propagate upward and outward prematurely [17]. This restriction causes a rapid escalation in effective stress within the immediate vicinity of the tip, leading to a surge in penetration resistance before the physical skirt tip has even breached the interface. Once the tip passes the interface, it must aggressively shear through the dense material, while the upper portion of the skirt continues to interact with the loose layer. Furthermore, the permeability contrast between the two layers creates a discontinuity in the hydraulic gradient during suction application. If the dense layer has a lower permeability, it can throttle the seepage flow, reducing the beneficial effective stress degradation that the suction is intended to provide, further compounding the resistance.

3.3 Formulation of Penetration Energy

Penetration energy is the definitive metric for assessing the cumulative difficulty of the installation process. It provides a holistic measure of the work done by the installation forces (self-weight and suction) to overcome the soil resistance over the entire depth of embedment. Mathematically, the penetration energy is the definite integral of the total penetration resistance force with respect to the depth of penetration.

$$E_{total} = \int_0^{D_f} F_p(z)dz$$

In a perfectly homogeneous soil, the force increases roughly linearly or parabolically with depth, leading to a predictable, smooth accumulation of total energy. However, due to the stress bulb interaction and seepage anomalies detailed above, the function governing the penetration force near an interface becomes highly non-linear [18]. The rate of energy accumulation, which is the derivative of the total energy curve, spikes dramatically within the interface transition zone. To accurately predict the total installation energy, theoretical models must be augmented with an interface influence function that modifies the baseline resistance equations based on the distance from the interface and the mechanical property contrast between the adjacent layers. This function accounts for the additional work required to deform the stiffer underlying layer and the work dissipated through altered seepage pathways.

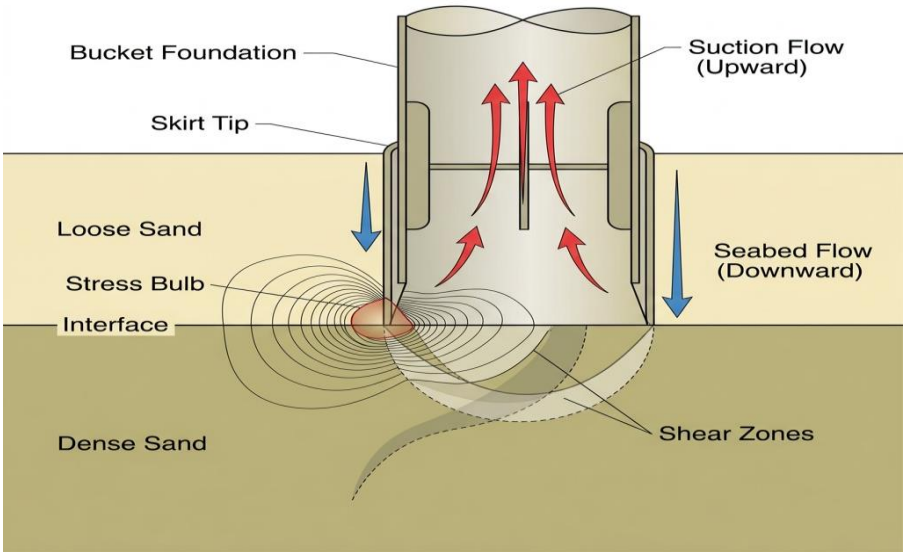


Figure 1: Comprehensive Schematic of Sand

4. Methodology and Experimental Setup

4.1 Design of Scaled Physical Models

To systematically investigate the influence of sand-layer interfaces on penetration energy, a comprehensive physical modeling program was designed and executed utilizing a large-scale geotechnical testing tank. The experimental apparatus consisted of a rigid, cylindrical steel tank with an internal diameter sufficiently large to minimize boundary effects and ensure that the stress field generated by the penetrating foundation model did not reflect off the tank walls. The model composite bucket foundation was fabricated from high-strength aluminum alloy to ensure rigidity while maintaining a manageable weight [19]. The model was geometrically scaled from a prototype multi-megawatt offshore wind turbine foundation, maintaining careful control over the aspect ratio (diameter to skirt length) and the skirt thickness to diameter ratio. To accurately capture the complex geometry of modern composite foundations, the model included an integrated transition piece and internal structural bulkheads. The foundation was attached to a high-precision, servo-hydraulic linear actuator capable of applying both displacement-controlled mechanical driving and force-controlled loading to simulate the self-weight phase. A sophisticated, closed-loop suction control system was plumbed into the top plate of the model bucket, utilizing a variable-frequency vacuum pump and electronic proportional valves to precisely regulate the internal pressure differential in real-time, thereby simulating the exact suction profiles utilized in full-scale offshore operations.

4.2 Soil Preparation and Characterization

The creation of the stratified sand beds required meticulous control over the pluviation process to ensure uniform relative densities within each layer and a distinctly defined horizontal interface between them. A highly uniform, fine-grained silica sand was selected as the testing medium due to its well-documented mechanical properties and consistent particle shape. The sand beds were prepared using a mechanized traveling sand rainer, which calibrates the drop height and the aperture size of the discharge hopper to control the impact energy of the falling sand particles, thereby dictating the final void ratio of the deposit. For each test, a dual-layer profile was constructed. The lower layer was systematically pluviated to achieve a high relative density state, simulating a stiff, competent marine bearing stratum. Once the lower layer reached the target elevation, the sand rainer was recalibrated, and the upper layer was pluviated at a lower drop height to achieve a loose relative density state, simulating unconsolidated surficial marine sediments [20]. The exact depth of the interface relative to the final target penetration depth of the foundation was varied across different test series to evaluate how the vertical position of the transition zone influences the overall energy accumulation. The geotechnical properties of the prepared sand states were rigorously characterized through standard laboratory procedures, including triaxial shear tests and constant-head permeability tests.

Table 1Geotechnical Properties of the Prepared Stratified Sand Profiles

Parameter	Loose Sand Layer	Dense Sand Layer	Testing Standard
Relative Density (%)	35.5	82.0	Standard Pluviation
Effective Unit Weight (kN/m^3)	9.42	10.85	Volume Displacement
Peak Friction Angle (degrees)	31.2	41.5	Consolidated Drained Triaxial
Permeability Coefficient (m/s)	1.8×10^{-4}	7.2×10^{-5}	Constant Head Method
Void Ratio (initial)	0.78	0.54	Gravimetric Analysis

4.3 Instrumentation and Data Acquisition Systems

An extensive array of precision sensors was deployed to capture the highly transient and localized phenomena occurring during the installation process, particularly as the foundation crossed the sand-layer interface. The primary vertical penetration force was continuously monitored using a high-capacity, low-profile load cell positioned between the hydraulic actuator and the foundation model. Vertical displacement was tracked using dual linear variable differential transformers (LVDTs) mounted symmetrically to eliminate rotational errors. To map the complex evolution of the pore water pressure regime, miniaturized pore pressure transducers (PPTs) were installed at multiple critical locations. Several PPTs were embedded flush with the internal and external surfaces of the foundation skirt to monitor dynamic seepage pressures along the soil-structure interface, while a vertical array of PPTs was pre-installed within the soil bed itself, traversing the planned interface zone to capture the migration of the hydraulic gradient. Additionally, ultra-thin tactile pressure sensors were affixed to the foundation skirt to provide real-time mapping of the normal stress and frictional resistance distribution as the skirt passed from the loose to the dense layer. All sensor data was routed through a multi-channel, high-speed data acquisition system logging at a high sampling frequency to ensure that the rapid changes in resistance and pressure occurring precisely at the interface breach were captured with high temporal resolution [21].

5. Computational Modeling and Analysis

5.1 Formulation of the Finite Element Framework

While the physical modeling program provided invaluable empirical data, a sophisticated computational framework was required to visualize the internal stress states, soil displacement trajectories, and exact mechanisms of energy dissipation that are inherently unobservable in a physical tank. A three-dimensional, fully coupled hydro-mechanical finite element model was constructed to simulate the penetration process. Given the extremely large deformations involved in foundation installation, traditional Lagrangian meshes suffer from severe element distortion, leading to numerical instability and premature termination of the analysis. To overcome this critical limitation, the Coupled Eulerian-Lagrangian (CEL) method was employed. In the CEL framework, the composite bucket foundation was modeled as a rigid Lagrangian body, which is computationally efficient and appropriate given the relative stiffness difference between the aluminum structure and the soil. The stratified sand bed was modeled as an Eulerian domain, wherein the soil material flows through a fixed background mesh. This approach entirely eliminates the problem of mesh entanglement while accurately capturing the large-scale volumetric displacement and the formation of the soil plug within the advancing bucket. The Eulerian domain was carefully discretized, with heavy mesh refinement implemented along the anticipated penetration path and specifically clustered at the designated elevation of the sand-layer interface to capture high stress gradients.

5.2 Constitutive Modeling and Interface Mechanics

The accurate representation of the sand behavior, particularly its density-dependent dilatancy and stress-dependent stiffness, is paramount for replicating the interface effects. A sophisticated elasto-plastic bounding surface plasticity model, specifically calibrated for granular materials under dynamic loading, was utilized. This constitutive model incorporates a state parameter approach, allowing it to seamlessly transition between the contractive behavior of the loose upper layer and the heavily dilatant behavior of the dense lower layer without requiring fundamentally different mathematical formulations for each stratum. The interaction between the steel foundation and the soil was governed by a robust general contact algorithm enforcing a strict penalty-based kinematic constraint. The frictional behavior at the soil-structure interface was defined using a classical Coulomb friction model modified to account for the continuous change in normal stress induced

by both the physical displacement and the seepage forces. The formulation for the interface shear stress is critical for energy calculations.

$$\tau = \sigma_n tan(\delta) + c_a$$

Where the effective normal stress and the interface friction angle govern the sliding resistance. Because the installation involves fluid flow, the computational model was fully coupled, solving the equilibrium equations and the fluid continuity equations simultaneously. The application of suction was simulated by defining a time-dependent boundary condition representing the negative pore pressure on the interior soil surface, driving fluid flow through the Eulerian mesh and actively modifying the effective stress field in response to the changing hydraulic gradients.

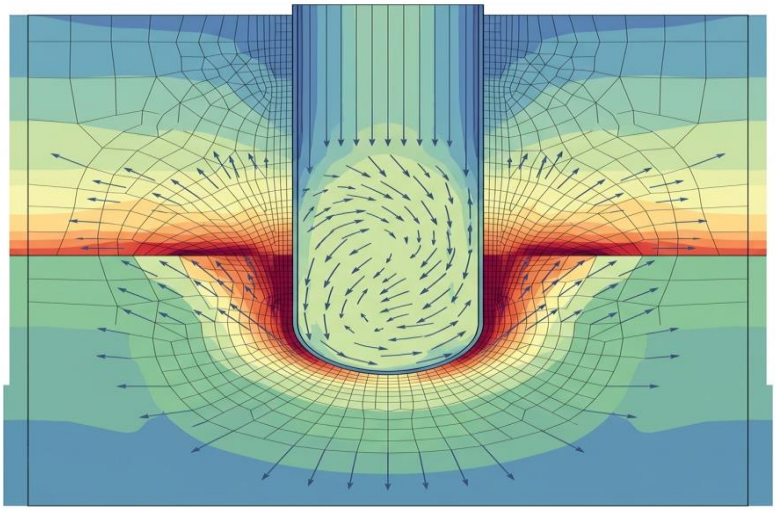


Figure 2: Advanced Computational Mesh and Stress Field Distribution

5.3 Boundary Conditions and Computational Execution

The boundary conditions of the computational domain were meticulously established to replicate the physical testing environment while optimizing computational efficiency. The lateral boundaries of the Eulerian domain were fixed against horizontal displacement but allowed vertical fluid flow, whereas the bottom boundary was fully fixed against displacement and designated as impermeable to simulate a rigid, deep bedrock layer. The initial geostatic stress state was established through a preliminary analysis step, applying gravity to the distinct layers to generate the correct initial effective stress and pore pressure profiles. The penetration process was simulated in small, explicit time increments to maintain numerical stability during the highly dynamic contact transitions. The analysis output continuous records of total reaction force, kinetic energy, plastic dissipation energy, and frictional work, which were subsequently extracted and integrated over the penetration depth to calculate the total penetration energy. By varying the depth of the interface and the magnitude of the applied suction in parametric studies, the computational model provided a vast dataset that was cross-referenced and validated against the physical experimental results.

6. Results and Discussion

6.1 Evolution of Penetration Resistance Across the Interface

The continuous logging of penetration resistance provided a clear, high-resolution picture of how the sand-layer interface disrupts the installation process. In the initial phase of installation through the upper loose sand layer, the resistance curve followed a predictable, slightly concave upward trajectory. The application of suction effectively degraded the tip resistance, and the required

driving force remained low. However, as the foundation skirt approached within approximately 0.5 to 0.7 times the foundation diameter from the interface boundary, a distinct inflection point was observed in the data. The penetration resistance began to escalate rapidly, deviating sharply from the theoretical homogeneous curve. This early warning effect is definitively attributed to the interaction between the downward-propagating stress bulb and the much stiffer dense sand layer below. The dense layer effectively acts as a rigid boundary, constraining the plastic flow of the loose sand and forcing a premature increase in effective stress at the foundation tip. As the physical tip of the skirt breached the interface, the resistance reached a localized maximum. Once fully embedded within the dense layer, the resistance curve stabilized onto a new, much steeper gradient characteristic of the high relative density and high friction angle of the lower stratum.

6.2 Analysis of Energy Accumulation and Dissipation

The integration of the resistance curves yielded the total penetration energy profiles, which clearly demonstrated the severe impact of stratified soils on installation efficiency. The data revealed that the total energy required to install the foundation to a target depth through the two-layer system was significantly greater than the energy required if the entire profile consisted of a homogenous mixture of the two densities.

Table 2Comparative Analysis of Penetration Energy Across Varying Interface Depths

Interface Depth Ratio (z/D)	Peak Resistance at Interface (kN)	Total Penetration Energy (kJ)	Deviation from Homogeneous Baseline (%)
0.25 (Shallow)	14.5	420.5	+ 12.4
0.50 (Intermediate)	28.2	585.3	+ 28.7
0.75 (Deep)	41.6	810.2	+ 45.1
1.00 (No Interface - Dense)	N/A	690.4	N/A
0.00 (No Interface - Loose)	N/A	210.8	N/A

The most critical finding from the energy analysis was the disproportionate energy consumption occurring exactly at the transition zone. The energy derivative—the rate of work done per millimeter of penetration—spiked dramatically as the skirt transitioned through the interface. This indicates that the installation equipment must possess significant reserve energy capacity to push through this barrier, even if the average strength of the total soil profile seems manageable. The computational models provided further insight, revealing that a massive proportion of the total mechanical work during this phase is dissipated as plastic deformation within the highly compressed stress bulb, rather than overcoming pure sliding friction. The dense layer refuses to yield easily, forcing the loose sand in the stress bulb into an extremely dense state before shear failure can propagate.

6.3 Seepage Alterations and Plug Stability

The presence of the dense underlying layer also profoundly affected the hydraulic mechanisms essential for suction installation. When the foundation tip was located in the loose layer, the applied suction generated a uniform and highly effective upward seepage flow, drastically reducing internal friction. However, as the interface was approached, the significantly lower permeability of the dense sand layer began to throttle the seepage flow. The pressure gradient became highly non-uniform, concentrating primarily in the loose material directly above the interface. This throttling effect meant that the beneficial reduction in effective stress provided by the suction was drastically reduced exactly when it was needed most—as the foundation attempted to penetrate the stiffer layer. This loss of hydraulic efficiency is a primary contributor to the observed spikes in

total penetration energy. Furthermore, the varying permeabilities caused differential lifting forces on the soil plug. The physical experiments showed evidence of minor internal localized boiling and piping in the loose sand immediately above the interface as the foundation struggled to advance, highlighting a significant stability risk if the operator attempts to overcome the resistance spike by simply increasing suction pressure beyond safe limits [22].

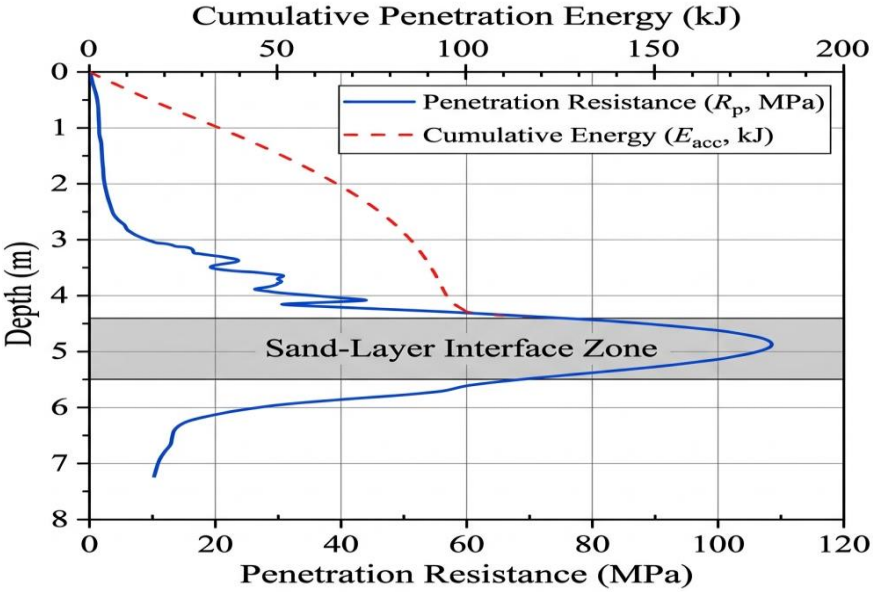


Figure 3Penetration Resistance and Energy Accumulation Profiles

7. Conclusion

7.1 Summary of Interface Dynamics

The installation of composite offshore bucket foundations in heterogeneous, stratified marine soils presents complex geotechnical challenges that deviate significantly from classical homogeneous design assumptions. This comprehensive investigation has demonstrated that the presence of a sand-layer interface—specifically transitioning from a loose surficial layer to a dense bearing stratum—has a profound and highly non-linear influence on both the instantaneous penetration resistance and the cumulative penetration energy. The interaction between the advancing foundation tip and the stiffer underlying stratum generates a severe stress concentration, effectively constraining the plastic flow of the soil and initiating a spike in resistance well before the physical boundary is reached. Concurrently, the contrast in hydraulic permeability between the strata significantly diminishes the efficiency of the suction-assisted seepage mechanism, depriving the installation process of the critical effective stress degradation required to advance the foundation.

7.2 Implications for Offshore Engineering Practice

The findings presented in this study hold critical implications for the design and deployment of offshore renewable energy infrastructure. The total penetration energy cannot be accurately predicted by simply averaging the properties of layered soils or by integrating piecewise homogeneous resistance functions. Ignoring the localized energy spikes at soil interfaces can lead to severe underestimation of required installation capacities, resulting in catastrophic premature refusal, equipment damage, or foundation buckling during offshore operations. The theoretical formulations and comparative data provided herein offer a more rigorous framework for evaluating layered seabed conditions. Future design methodologies must incorporate specific interface transition modifiers to calculate energy accumulation accurately. By enhancing our predictive capabilities regarding complex soil-structure interactions, the offshore engineering community can optimize the structural design of composite foundations, tailor installation protocols to specific

geological site conditions, and ultimately accelerate the safe and economical expansion of offshore wind energy in highly challenging deep-water environments.

References

Zhang, J., Peng, H., Sun, L., Wu, G., Liu, C., & Yu, Z. (2025, August). Unsupervised graph clustering with deep structural entropy. In Proceedings of the 31st ACM SIGKDD Conference on Knowledge Discovery and Data Mining V. 2 (pp. 3752-3763).

Ouyang, Z., & Mayne, P. W. (2020). Effective Stress Friction Angle of Normally Consolidated and Overconsolidated Intact Clays from Piezocone Tests. Geotechnical Engineering (0046-5828), 51(2), 111.

Ouyang, Z., Mayne, P. W., & Agaiby, S. (2024). In situ test-based evaluation of soil effective stress strength properties and stress history. In Databases for Data-Centric Geotechnics (pp. 344-368). CRC Press.

Agaiby, S. S., Ouyang, Z., & Mayne, P. W. (2018). Helical probe tests in residual soils of the Appalachian Piedmont. Geomechanics and Geoengineering, 13(3), 217-225.

Li, Y. Z., Zhang, J. P., Chen, Z. Y., Wang, H. C., Zhang, K. X., Hu, S. S., ... & Dudley, M. (2026, September). Growth and Characterization of High-Quality Thick Epitaxial 4H-SiC Wafers for High Voltage Devices. In Defect and Diffusion Forum (Vol. 452, pp. 79-85). Trans Tech Publications Ltd.

Li, X., Wang, P., Li, G., & Zhang, Y. (2023). Design of a novel self-test-on-chip interface ASIC for capacitive accelerometers. IEEE Transactions on Circuits and Systems I: Regular Papers, 70(7), 2834-2843.

Xiong, S., Chen, T., Rupendra, A., Clement, C., Gasparri, E., & Lucchi, E. (2026). Embodied Carbon of Progressive Timber Integration in a 47-Storey Tropical High-Rise: A Singapore Public Housing Case Study. Building and Environment, 114910.

Yu, A., Pang, F., Yuan, Y., Huang, Y., Li, S., Yu, S., ... & Xia, L. (2023). Simultaneous current and vibration measurement based on interferometric fiber optic sensor. Optics & Laser Technology, 161, 109223.

Zhang, S., Zhang, E., Cookson, J., Huang, P., & Yan, W. (2026). A hybrid XFEM-calibrated analytical framework for efficient fatigue crack growth prediction. International Journal of Fatigue, 109682.

Zhang, S., Huang, P., & Yan, W. (2024). A data-driven approach for railway in-train forces monitoring. Advanced Engineering Informatics, 59, 102258.

Wang, Y., Lou, M., Liang, W., & Zhang, C. (2023). Numerical and experimental investigation on tensile fatigue performance of reinforced thermoplastic pipes. Ocean Engineering, 287, 115814.

Huang, S., Wang, X., Qu, T., & Liu, C. (2024). Torque curve bifurcation in T-shaped rotor continuously drilling into granular media. Powder Technology, 444, 119947.

Zhao, R., Tang, J., Zeng, W., Chen, Z., & Zhao, X. (2024, October). Zero-shot knowledge graph question generation via multi-agent llms and small models synthesis. In Proceedings of the 33rd ACM International Conference on Information and Knowledge Management (pp. 3341-3351).

Li, Q., Ye, Q., Zhang, N., Zhang, W., & Hu, F. (2025). Digital-twin-enabled industrial IoT: Vision, framework, and future directions. IEEE Wireless Communications, 32(6), 173-181.

Li, S. (2025). Momentum, volume and investor sentiment study for us technology sector stocks—A hidden markov model based principal component analysis. PloS one, 20(9), e0331658.

Li, X., Wang, P., Li, G., Ni, L., & Zhang, Y. (2023). Design of interface circuits and lightweight PUF for TMR sensors. IEEE Sensors Journal, 23(11), 11754-11761.

Liu, X., Yu, Z., Yao, Y., Yang, K., Zeng, H., & Chen, C. P. (2026). A Comprehensive Survey of Cross-Modal Retrieval: Breaking Through Modal Barriers. ACM Computing Surveys.

Zhang, Q., Yang, M., Sun, G., Xiang, Y., Wang, S., Zhang, J., & Li, S. (2026). Representation learning accelerates the development of models for Li-ion battery health diagnostics and prognostics. Energy Storage Materials, 104897.

Yang, Z., Ji, W., & Wang, Z. (2024). Adaptive joint configuration optimization for collaborative inference in edge-cloud systems. Science China Information Sciences, 67(4), 149103.

Chai, L., Zhang, J., Li, H., Cui, C., Jiang, J., Zheng, B., ... & Jiang, L. (2021). Investigation of thermomorphogenesis-related genes for a multi-silique trait in Brassica napus by comparative transcriptome analysis. Frontiers in Genetics, 12, 678804.

Jia, Y., Wang, T., Xiao, K., & Guo, C. (2020). How to reduce opportunism through contractual governance in the cross-cultural supply chain context: evidence from Chinese exporters. Industrial Marketing Management, 91, 323-337.

Xu, Y. (2020). A review of machine learning with echo state networks. Proj. Rep.